

Non-reciprocity across scales in active mixtures

Alberto Dinelli,¹ Jérémy O’Byrne,^{1,2} Agnese Curatolo,³ Yongfeng Zhao,⁴ Peter Sollich,^{5,6} and Julien Tailleur^{1,7}

¹*Université Paris Cité, Laboratoire Matière et Systèmes Complexes (MSC), UMR 7057 CNRS, F-75205, 75205 Paris, France*

²*Department of Applied Maths and Theoretical Physics, University of Cambridge, Centre for Mathematical Sciences, Wilberforce Rd, Cambridge CB3 0WA, UK*

³*John A. Paulson School of Engineering and Applied Sciences and Kavli Institute for Bionano Science and Technology, Harvard University, Cambridge, MA 02138, USA*

⁴*Center for Soft Condensed Matter Physics and Interdisciplinary Research & School of Physical Science and Technology, Soochow University, 215006 Suzhou, China*

⁵*Institute for Theoretical Physics, Georg-August-Universität Göttingen, 37 077 Göttingen, Germany*

⁶*Department of Mathematics, King’s College London, London WC2R 2LS, UK*

⁷*Department of Physics, Massachusetts Institute of Technology, Cambridge, Massachusetts 02139, USA*

(Dated: December 26, 2022)

In active matter, the lack of momentum conservation makes non-reciprocal interactions the rule rather than the exception. They lead to a rich set of emerging behaviors that are hard to account for and to predict starting from the microscopic scale, due to the absence of a generic theoretical framework out of equilibrium. Here we consider bacterial mixtures that interact via mediated, non-reciprocal interactions like quorum-sensing and chemotaxis. By explicitly relating microscopic and macroscopic dynamics, we show that non-reciprocity may fade as coarse-graining proceeds, leading to large-scale bona fide equilibrium descriptions. In turns, this allows us to account quantitatively, and without fitting parameters, for the rich behaviors observed in microscopic simulations including phase separation, demixing or multi-phase coexistence. We also derive the condition under which non-reciprocity is strong enough to survive coarse-graining, leading to a wealth of dynamical patterns. Again, the explicit coarse-graining of the dynamics allows us to predict the phase diagram of the system starting from its microscopic description. All in all, our work demonstrates that the fate of non-reciprocity across scales is a subtle and important question.

INTRODUCTION

Our ability to design and engineer new materials largely relies on the possibility to infer their large-scale properties from their microscopic constituents. For equilibrium systems, statistical mechanics allows us to do so by relating the macroscopic free energy to the microscopic partition function and the Boltzmann weight. As a result, the emerging properties of equilibrium systems can be predicted by balancing energy and entropy. This general principle, at the root of so many industrial innovations over the past century, comes with a strong restriction: it only applies to the steady state of systems satisfying detailed balance, thus excluding the vast class of nonequilibrium systems and transient dynamical phenomena. An important challenge is thus to develop theoretical frameworks that would allow us to relate the microscopic description of nonequilibrium systems to their emerging behavior.

This is particularly important for active systems, which comprise large assemblies of individual units able to exert non-conservative forces on their environment [1]. From spontaneously flowing matter [2–5] to living crystals [6–10], active materials display phases without counterparts in equilibrium physics [11]. This rich phenomenology relies in part on the existence of non-reciprocal interactions (NRI) between active particles, which have attracted a lot of attention recently. From the spontaneous emergence of traveling waves to anomalous mechanics and odd elasticity, NRI have indeed been shown to lead to a wealth of exciting phenomena [12–25].

In the simplest case of systems with pairwise forces, NRI

correspond to the breakdown of Newton’s third law, which states that if particle i exerts a force \mathbf{f}_{ij} onto particle j then $\mathbf{f}_{ji} = -\mathbf{f}_{ij}$. Active systems exchange momentum with their environment and are thus free of this constraint. Note that pairwise forces are an idealized limit for most active particles: experimental systems instead typically involve complex mediated N -body interactions like chemotaxis, quorum sensing, or hydrodynamic interactions. In all cases, predicting how such microscopic interactions impact the emerging behavior is a challenging, indeed mostly impossible task. An appealing alternative has recently been proposed: to postulate phenomenological theories in which action/reaction is directly broken at the macroscopic scale [16, 17]. The analysis of the large-scale behavior then amounts to a non-linear dynamics problem for which a wealth of tools are available [16, 17, 22, 23, 26–30]. However, a major limitation is that, in the presence of NRI, there is no generic way to infer which microscopic systems correspond to a given macroscopic description. This not only prevents us from assessing the scope of these theories, but it also deprives us of guiding principles when it comes to engineering microscopic active systems to realize the exciting emerging behaviors observed at the macroscopic scale.

In this article, we bridge the gap between microscopic and macroscopic descriptions of active systems with non-reciprocal interactions, which allows us to show that the violation of action-reaction is strongly scale dependent. To do so, we study active mixtures, which comprise several types of interacting active particles and have attracted a lot of interest recently [12, 16, 17, 21–24, 31–43]. We consider active

particles that interact via quorum sensing (QS), i.e. regulate their motility according to the local density of their peers. QS is generic in nature [44], where it is typically mediated by diffusing signalling molecules. For microorganisms, it plays an important role in regulating diverse biological functions, from bioluminescence [45–48] and virulence [49] to biofilm formation [50] and swarming [51]. Furthermore, QS can also be engineered in the lab, for instance using light-controlled self-propelled colloids [52–54].

We consider N ‘species’ of active particles and denote by $\rho_\mu(\mathbf{r})$ the density field of species μ . For concreteness, we present our results for active Brownian particles (ABPs) and run-and-tumble particles (RTPs), but we stress that they hold more generally and also apply, for instance, to active Ornstein-Uhlenbeck particles. QS interactions between the species then lead to the following dynamics for particle i of species μ :

$$\dot{\mathbf{r}}_{i,\mu} = v_\mu(\mathbf{r}_i, [\{\rho_\nu\}]) \mathbf{u}_{i,\mu}, \quad (1)$$

where the self-propulsion speed v_μ is both a function of \mathbf{r}_i and a functional of all density fields. The particle orientation $\mathbf{u}_{i,\mu}$ is a unit vector that undergoes either rotational diffusion (ABPs) or tumbles instantaneously (RTPs), with a persistence time τ_μ [55]. We note that Eq. (1) is non-reciprocal by definition: the displacements of particles i and j of species μ and ν impact their respective velocities in completely arbitrary ways. To address how this non-reciprocity affects the large-scale properties, we first coarse-grain the dynamics (1). We then compute the entropy production rate of the resulting fluctuating hydrodynamics and show that it *vanishes* whenever

$$\frac{\delta \log v_\mu(\mathbf{r})}{\delta \rho_\nu(\mathbf{r}')} = \frac{\delta \log v_\nu(\mathbf{r}')}{\delta \rho_\mu(\mathbf{r})} \quad \text{for any } \mu, \nu. \quad (2)$$

In this case, the microscopic non-equilibrium dynamics leads to an effective large-scale equilibrium theory and non-reciprocity vanishes upon coarse-graining. To the best of our knowledge, condition (2) is the first non-trivial generalization of Newton’s action-reaction principle to a microscopic model of active mixtures in the presence of many-body mediated interactions. We show that the system then admits an effective free energy which allows predicting its emerging behavior. Remarkably, this allows us to construct the phase diagram of the system from its microscopic dynamics without any fit parameters, a rare achievement even in equilibrium. On the contrary, when Eq. (2) is violated, non-reciprocity survives coarse-graining and we derive a sufficient condition on the *microscopic* dynamics to observe travelling patterns that explicitly break time-reversal symmetry at the macroscopic scale. All in all, our work thus demonstrates that the fate of non-reciprocity across scales is a subtle and important question. To support the generality of this statement, we close our article by extending our results to chemotactic interactions where macroscopic reciprocity may again emerge despite microscopic NRI.

FLUCTUATING HYDRODYNAMICS

We start by coarse-graining the microscopic dynamics (1) in the presence of QS interactions. The hydrodynamic modes are the fluctuating conserved density fields $\rho_\mu(\mathbf{r}) = \sum_j \delta(\mathbf{r} - \mathbf{r}_{j,\mu})$. As shown in the Supplementary Information, the dynamics in d space dimensions can be obtained as N coupled Itô-Langevin equations:

$$\partial_t \rho_\mu = -\nabla_{\mathbf{r}} \cdot [\mathbf{V}_\mu \rho_\mu - D_\mu \nabla_{\mathbf{r}} \rho_\mu + \sqrt{2D_\mu \rho_\mu} \mathbf{\Lambda}_\mu], \quad (3)$$

where the $\mathbf{\Lambda}_\mu(\mathbf{r}, t)$ are independent Gaussian white noise fields of zero mean, unit variance, and independent components. The collective diffusivities and drifts then read

$$D_\mu = \frac{v_\mu^2(\mathbf{r}, [\{\rho_\nu\}]) \tau_\mu}{d}, \quad \mathbf{V}_\mu = -D_\mu \nabla \log[v_\mu(\mathbf{r}, [\{\rho_\nu\}])]. \quad (4)$$

Inspection of Eq. (3) shows that it can be rewritten as

$$\partial_t \rho_\mu = \nabla_{\mathbf{r}} \cdot [M_\mu \nabla \mathbf{u}_\mu + \sqrt{2M_\mu} \mathbf{\Lambda}_\mu], \quad (5)$$

where $M_\mu(\mathbf{r}) = \rho_\mu(\mathbf{r}) D_\mu(\mathbf{r}, [\{\rho_\nu\}])$ is a density-dependent collective mobility and $\mathbf{u}_\mu(\mathbf{r}) = \log[\rho_\mu(\mathbf{r})] + \log[v_\mu(\mathbf{r}, [\{\rho_\nu\}])]$ is an effective chemical potential. One can then study the large-scale behavior of the system using Eq. (5) and connect it to the microscopic dynamics using Eqs. (4).

WHEN NON-RECIPROcity VANISHES UPON COARSE-GRAINING

Note that the fluctuating hydrodynamics (5) takes a form reminiscent of N coupled model-B dynamics [56] and it is thus natural to ask whether we have coarse-grained our microscopic model into an effective equilibrium one. To address this question, we show in the Supplementary Information that the stochastic dynamics (5) leads to an entropy production rate given by:

$$\sigma = \int d^d \mathbf{r} \sum_{\mu=1}^N \left\langle M_\mu \left[\nabla \left(\mathbf{u}_\mu + \frac{\delta \log P_s}{\delta \rho_\mu(\mathbf{r})} \right) \right]^2 \right\rangle, \quad (6)$$

where $P_s[\{\rho_\nu(\mathbf{r})\}]$ is the steady-state distribution. Equation (6) relates the irreversibility of the system at the macroscopic scale to its microscopic parameters $\{v_\nu\}$ through $\mathbf{u}_\mu = \log v_\mu + \log \rho_\mu$. For generic QS interactions, σ is positive and the coarse-grained dynamics is out of equilibrium. However, the model admits a macroscopic equilibrium limit whenever there exists a functional $\mathcal{F}[\{\rho_\nu\}]$ such that $\mathbf{u}_\mu(\mathbf{r}) = \frac{\delta \mathcal{F}}{\delta \rho_\mu(\mathbf{r})}$. It is then easy to check that $P_s \propto \exp[-\mathcal{F}]$ and that σ vanishes. Furthermore, \mathcal{F} is mathematically equivalent to a free energy in equilibrium and plays the role of a Lyapunov functional for the dynamics, since $\partial_t \langle \mathcal{F} \rangle = -\int d\mathbf{r} \sum_\mu \langle M_\mu (\nabla \frac{\delta \mathcal{F}}{\delta \rho_\mu})^2 \rangle < 0$.

To assess whether such an effective free energy exists, we need to determine the conditions under which \mathbf{u}_μ can be written as a functional derivative. To do so, we generalize the

functional Schwarz theorem [1] to the case of N coupled stochastic field equations. As shown in the Supplementary Information, this leads to a system of N^2 equations in the sense of distributions:

$$\forall(\mu, \nu), \quad \mathcal{D}_{\mu\nu}(\mathbf{r}, \mathbf{r}') \equiv \frac{\delta u_\mu(\mathbf{r})}{\delta \rho_\nu(\mathbf{r}')} - \frac{\delta u_\nu(\mathbf{r}')}{\delta \rho_\mu(\mathbf{r})} = 0. \quad (7)$$

Using the explicit expression for the chemical potential u_μ then directly leads to the condition (2) for the microscopic dynamics. When the self-propulsion depends exclusively on local densities, *i.e.* $v_\mu(\mathbf{r}) \equiv v_\mu(\rho_1(\mathbf{r}), \dots, \rho_N(\mathbf{r}))$, Equation 7 simplifies to

$$\frac{\partial \log v_\mu}{\partial \rho_\nu} = \frac{\partial \log v_\nu}{\partial \rho_\mu}, \quad (8)$$

whose full solution space can be constructed explicitly. Indeed, the solutions to Eq. (8) are generated by the gradient in ρ_μ -space of all the ‘potentials’ $U(\rho_1, \dots, \rho_N)$ through $\log v_\mu = \frac{\partial U}{\partial \rho_\mu}$. The effective free energy can then be directly computed as

$$\mathcal{F}[\{\rho_\mu\}] = \int d\mathbf{r} f(\mathbf{r}) \quad (9a)$$

$$f(\mathbf{r}) = U(\{\rho_\mu(\mathbf{r})\}) + \sum_\mu \rho_\mu(\mathbf{r}) \log \rho_\mu(\mathbf{r}). \quad (9b)$$

Importantly, even though the microscopic dynamics then maps onto a *bona fide* equilibrium problem at the macroscopic scale, the contribution of particle (i, μ) to the velocity $\dot{\mathbf{r}}_{j,\nu}$ of particle (j, ν) is *not* equal and opposite to the contribution of particle (j, ν) to $\dot{\mathbf{r}}_{i,\mu}$. In other words, momentum conservation is still violated at the microscopic scale and the interactions are still non-reciprocal. Equation (8) can then be seen as a non-trivial *microscopic constraint* on the QS interactions such that action-reaction is restored at the *macroscopic scale*.

Let us now show how our effective equilibrium theory allows us to account for the emerging behaviors of binary active mixtures when equation (2) is satisfied. For sake of generality, we allow both for global interactions, where the self-propulsion speed v_μ of species μ depends on the total density field of particles, $\rho_t(\mathbf{r}) = \sum_\mu \rho_\mu(\mathbf{r})$, and for specific ones, where v_μ depends specifically on one—or more—density field $\rho_\nu(\mathbf{r})$. In the latter case, we refer to self and cross interactions when $\mu = \nu$ and $\mu \neq \nu$, respectively. We consider self-inhibition of motility coupled to a global enhancement of motility through

$$v_\mu(\mathbf{r}) = v_\mu^0 \phi_\mu^s[\tilde{\rho}_\mu(\mathbf{r})] \phi_\mu^g[\tilde{\rho}_t(\mathbf{r})]. \quad (10)$$

In Eq. (10), self and global regulations are modelled by sigmoidal functions ϕ_μ^s and ϕ_μ^g , respectively, and $\tilde{\rho}(\mathbf{r}) = K * \rho(\mathbf{r})$ is a local measurement of the density field obtained by convolution with a kernel K (see Supplementary Information for details). Note that QS interactions leading to Eq. (10) can actually be realized using orthogonal QS circuits starting from clonal bacterial strains [57]. The non-local sampling of

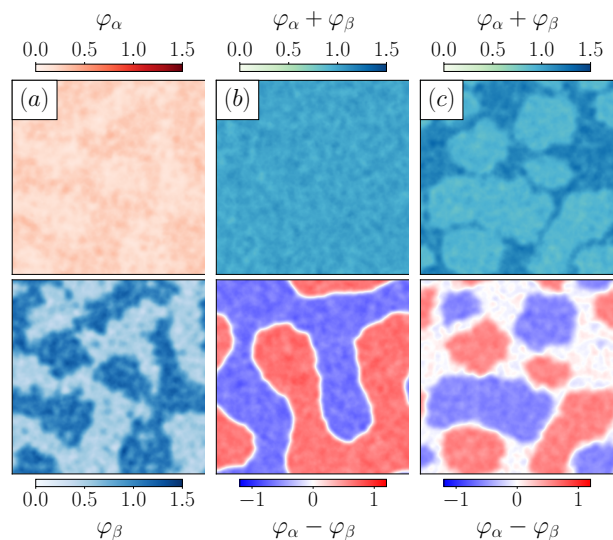


FIG. 1. Simulations of two species of RTPs with self-inhibition and global activation of the motility as in Eq. (10), for different average densities $\rho_{\alpha,\beta}^0$. Normalized densities are defined as: $\varphi_\mu = \rho_\mu / (\rho_\alpha^0 + \rho_\beta^0)$. (a) Phase separation of species β ($\rho_\alpha^0 = 15, \rho_\beta^0 = 50$). (b) Demixing ($\rho_{\alpha,\beta}^0 = 55$). (c) Triple coexistence between α -rich, β -rich, and well-mixed phases ($\rho_{\alpha,\beta}^0 = 75$). All parameters and numerical details are given in Supplementary Information.

the density then results from a fast variable treatment on the signalling molecular field [58]. Alternatively, such interactions can be directly engineered for light-controlled active colloids [52, 53]. Self-inhibition and global activation of motility then correspond to $\partial_{\tilde{\rho}} \phi_\mu^s < 0$ and $\partial_{\tilde{\rho}} \phi_\mu^g > 0$, respectively. To map out the phases accessible to the system, we carried out large-scale simulations of dynamics (1) using the QS interactions (10), as described in Supplementary Information.

Varying the overall composition of the system reveals a rich phenomenology. First, as in single-species systems, the self-inhibition of a given species may lead to its motility-induced phase separation [59, 60]. The second species then experiences a mild opposite modulation of its density field (Fig. 1a). Then, two phases specific to (active) mixtures emerge from the global coupling. First, Fig. 1b shows a segregated phase in which the two strains demix and undergo phase separation. Note that the global density field $\rho_t(\mathbf{r})$ remains homogeneous, contrary to what happens in the case of single-species phase separation shown in Figs 1a and S1. Second, Fig. 1c shows the existence of a triple-coexistence regime leading to the joint observation of α -rich, β -rich, and well-mixed phases, together with an overall phase-separation for $\rho_t(\mathbf{r})$. Let us now show how our effective equilibrium theory allows us to account for the phase diagram of the system quantitatively.

Under the local approximation $\tilde{\rho}_\mu(\mathbf{r}) \simeq \rho_\mu(\mathbf{r})$, Eq. (10) leads to $\log v_\mu = \log v_\mu^0 + \log \phi_\mu^s(\rho_\mu) + \log \phi_\mu^g(\rho_t)$. Direct inspection shows that Eq. (8) then amounts to $\phi_\mu^g = \phi_\nu^g$

for all μ, ν : the sole requirement for effective equilibrium is that the global interaction term ϕ_μ^g be common to all species. This is the case for the system shown in Fig. 1a-c, which can thus be mapped onto an equilibrium problem. The self-organization of the two coexisting species can then be predicted from the analysis of the corresponding effective free energy, which we detail in the Supplementary Information. Departure from a homogeneous, well-mixed system will occur whenever the free energy density (9b) is not convex. Predicting the coexisting densities then amounts to constructing the tangent planes of $f(\rho_\alpha, \rho_\beta)$ [61], as detailed in the Supplementary Information. In Fig. 2a, we compare these theoretical predictions to direct measurements for the parameters corresponding to Fig. 1a-c. Despite the construction relying on a locality assumption and a mean-field approximation, the agreement between predicted and measured phase diagrams in the composition space $(\rho_\alpha^0, \rho_\beta^0)$ is excellent. The triple coexistence regime reported in Fig. 1c emerges when the free energy surface admits a plane that is tangent in three points $(\rho_\alpha^i, \rho_\beta^i)_{i \in \{1,2,3\}}$ simultaneously, as illustrated in Fig. 2b. The corresponding compositions then delimit the coexistence region and determine the coexisting phases, while the respective fraction of each phase is obtained using the lever rule. Finally, the existence of an effective free energy also ensures that the Gibbs phase rule applies, which explains the existence of the three-phase and two-phase coexistence regions for our active binary mixture. The equilibrium mapping thus fully accounts for the static phase-separation scenario reported in Fig. 1. We now illustrate how violations of the microscopic condition (8) may lead to an emerging physics that explicitly breaks time-reversal symmetry.

WHEN NON-RECIPROCAL INTERACTIONS SURVIVE COARSENING

The violation of Eq. (2) is a sufficient condition for the emergence of non-reciprocal couplings between the density fields at the macroscopic scale (5). Consequently, the entropy production rate (6) is positive. The lack of a gradient structure for hydrodynamic equations is well known to allow for the existence of travelling patterns [16, 17, 21–23, 27, 28, 62]. To determine the *microscopic* condition for these to emerge, we consider the fate of perturbations around homogeneous solutions of Eq. (5), $\rho_\mu(\mathbf{r}) = \rho_\mu^0 + \delta\rho_\mu(\mathbf{r})$. In Fourier space, their linearized dynamics read $\partial_t \delta\hat{\rho}_\mu(\mathbf{q}) = -\mathbf{q}^2 \mathcal{M}_{\mu\nu}(\mathbf{q}) \delta\hat{\rho}_\nu$, with

$$\mathcal{M}_{\mu\nu}(\mathbf{q}) = D_\mu^0 \left[\delta_{\mu\nu} + \rho_\mu^0 \frac{\partial}{\partial \rho_\mu} \log v_\mu \right] \quad (11)$$

To do so, we carry out simulations of a two-species system with self-inhibition of motility and non-reciprocal cross-interactions given by

$$v_\mu(\mathbf{r}) = v_\mu^0 \phi_\mu^s[\tilde{\rho}_\mu(\mathbf{r})] \phi_\mu^c[\tilde{\rho}_\nu(\mathbf{r})]. \quad (14)$$

To control the strength of the non-reciprocal couplings, we chose $\phi_\mu^c(\tilde{\rho}) = \exp[\kappa_\mu^c \mathcal{S}_\mu^c(\tilde{\rho})]$, where $\mathcal{S}_\mu^c(\tilde{\rho})$ is a sigmoidal function described in Supplementary Information, and we

where $D_\mu^0 \equiv D_\mu(\{\rho_\nu^0\})$. As shown in Supplementary Information, for $N = 2$ species, eigenvalues with non-vanishing imaginary parts require

$$\frac{\partial v_\beta}{\partial \rho_\alpha} \frac{\partial v_\alpha}{\partial \rho_\beta} < -\frac{v_\alpha v_\beta (\mathcal{M}_{\alpha\alpha} - \mathcal{M}_{\beta\beta})^2}{4D_\alpha^0 D_\beta^0 \rho_\alpha^0 \rho_\beta^0}. \quad (12)$$

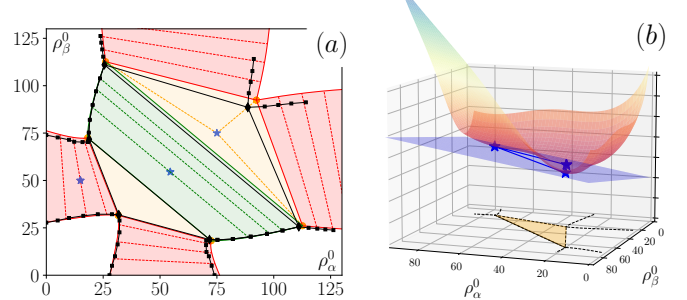


FIG. 2. (a) Phase diagram of two species of RTPs experiencing self-inhibition and global activation of motility according to Eq. (10). White regions correspond to homogeneous well mixed phases. Red, green, and ochre regions indicate one-species phase separation, demixing, and triple phase coexistence, respectively. Stars correspond to snapshots shown in Fig. 1a-c. Coexistence lines (solid) and tie-lines (dashed) are predicted using a tangent plane construction on the free energy density $f(\rho_\alpha, \rho_\beta)$ as detailed in the Supplementary Information. Black squares show coexisting densities measured in simulations. (b) Plot of the free energy density in the triple coexistence regime from Fig. 1c. The points where the tangent plane in blue touches the surface determine the three compositions that will be observed in the coexistence region.

We thus predict an oscillatory behavior in the presence of sufficiently strong, opposite interactions, e.g. when species β enhances the speed of α while α inhibits the motility of β . Under this condition, which is a stronger requirement than simple non-reciprocity, homogeneous profiles are linearly unstable whenever

$$\sum_{\mu=\alpha,\beta} D_\mu^0 \left(1 + \rho_\mu^0 \frac{\partial}{\partial \rho_\mu} \log v_\mu \right) < 0. \quad (13)$$

This opens up the possibility of travelling patterns, which we now explore.

We vary the values of κ_μ^c . We use self-inhibitions strong enough for Eq. (13) to hold so that the system is never homogeneous. As show in Figure 3, our simulations reveal a variety of static and dynamical patterns. In agreement with our prediction (12), travelling patterns are observed when $\kappa_\alpha^c \kappa_\beta^c < 0$ (orange quadrants). An intuitive microscopic understanding of the observed phases can be achieved by noticing that each species tends to accumulate where it goes more slowly [63–

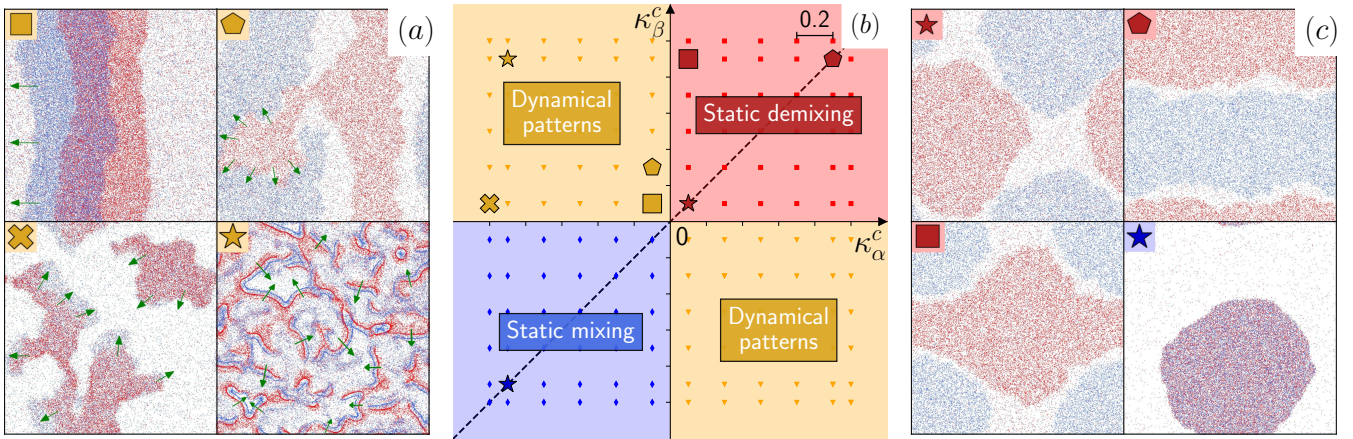


FIG. 3. Microscopic simulations of Eq. (14), with self-inhibition and non-reciprocal cross interactions. Panels (a) and (c) show the dynamical and static patterns observed in simulations, respectively; α -particles are depicted in red, β -particles in blue. The snapshots correspond to the larger symbols shown in panel (b). (b) Phase diagram as the couplings κ_α^c and κ_β^c are varied, where we remind that $\kappa_\mu^c > 0$ corresponds to the activation of the motility of species μ by the density of species ν , whereas $\kappa_\mu^c < 0$ corresponds to an inhibition. The background colors correspond to the prediction of linear stability analysis which are confirmed by numerical simulations (small symbols). The phase diagram is symmetric with respect to the dashed line $\kappa_\beta^c = \kappa_\alpha^c$ upon inverting the roles of α - and β -particles in panel (a,c). See Supplementary Information for other parameters and numerical details.

68]. Motility inhibition then acts as an effective attraction whereas motility enhancement leads to effective repulsion. When $\kappa_{\alpha,\beta}^c$ are both positive, the species effectively repel each other, leading to a triple coexistence regime with demixing between the dense phases (red quadrant). On the contrary, negative $\kappa_{\alpha,\beta}^c$ lead to effective attractive interactions and colocalization of the liquid phases (blue quadrant). The frustrated case, $\kappa_\alpha^c \kappa_\beta^c < 0$, corresponds to the motility of one species—say α —being inhibited by the other— β in this case—while that of β is enhanced by α . This leads to a complex run-and-chase dynamics between the two species that results in steady (orange square) or chaotic (orange star) travelling bands when $|\kappa_\alpha^c| \simeq |\kappa_\beta^c|$, as well as to a rich variety of more complex dynamical behaviors in less symmetric cases (orange cross and pentagon as well as SI movie 3-5). Thanks to the explicit coarse-graining of the microscopic dynamics, we are thus able to determine the microscopic condition for travelling patterns to emerge and to identify the mechanism leading to the run-and-chase dynamics.

NON-RECIPROCITY IN CHEMOTAXIS.

To show how our results generalize beyond the case of quorum sensing, we consider chemotactic interactions which have attracted a lot of interest in the context of bacterial suspensions [69–76]. For sake of generality, we consider N species of ABPs/RTPs that evolve according to the dynamics (1) and whose motilities are biased by the gradients of n chemical fields $\{c_p(\mathbf{r})\}$. We allow both for biases on the reorientation

dynamics and on the self-propulsion speeds:

$$v_\mu = v_{0\mu} - \mathbf{u}_{i,\mu} \cdot \sum_{p=1}^n v_{1\mu}^p \nabla_{\mathbf{r}_{i,\mu}} c_p, \quad (15)$$

$$\tau_\mu^{-1} = \tau_{0\mu}^{-1} + \mathbf{u}_{i,\mu} \cdot \sum_{p=1}^n (\tau_{1\mu}^p)^{-1} \nabla_{\mathbf{r}_{i,\mu}} c_p,$$

where the parameters $v_{*\mu}$, $\tau_{*\mu}^{-1}$ are constant. When $v_{1\mu}^p$, $\tau_{1\mu}^p$ are positive, particles increase their persistence lengths when moving towards minima of c_p , implying that c_p acts as a chemorepellent. Conversely, negative values of $v_{1\mu}^p$, $\tau_{1\mu}^p$ correspond to chemoattraction. We consider the case in which the chemicals are produced by the particles before they diffuse and degrade in the environment at non-vanishing rates. In the large system-size limit, the dynamics of c_p is thus much faster than that of the conserved density field ρ_μ and the chemical fields follow the evolution of the density fields adiabatically: $c_p(\mathbf{r}) \equiv c_p(\mathbf{r}, [\{\rho_\nu\}])$.

We start by coarse-graining the microscopic dynamics into a stochastic field theory for the density fields, which takes the form of Eq. (5) with an effective chemical potential given by (see Supplementary Information):

$$\mathbf{u}_\mu = \frac{1}{v_{0\mu}} \sum_{p=1}^n \left(\frac{v_{1\mu}^p}{\tau_{0\mu}} + \frac{v_{0\mu}}{\tau_{1\mu}^p} \right) c_p + \log \rho_\mu. \quad (16)$$

Consequently, the entropy production rate remains given by Eq. (6) albeit with \mathbf{u} determined by Eq. (16). The integrability condition for non-reciprocity to vanish across scales is then

given by the functional Schwarz theorem as:

$$\forall(\mu, \nu), \quad \frac{1}{v_{0\mu}^2} \sum_{p=1}^n \left(\frac{v_{1\mu}^p}{\tau_{0\mu}} + \frac{v_{0\mu}}{\tau_{1\mu}^p} \right) \frac{\delta c_p(\mathbf{r})}{\delta \rho_\nu(\mathbf{r}')} = \frac{1}{v_{0\nu}^2} \sum_{p=1}^n \left(\frac{v_{1\nu}^p}{\tau_{0\nu}} + \frac{v_{0\nu}}{\tau_{1\nu}^p} \right) \frac{\delta c_p(\mathbf{r}')}{\delta \rho_\mu(\mathbf{r})}. \quad (17)$$

Equation (17) determines when a microscopic chemotactic dynamics admits a large-scale effective equilibrium description.

For sake of concreteness, let us consider the simplest case of a single chemical field ($n = 1$) given by:

$$c(\mathbf{r}, [\{\rho_\nu\}]) = \sum_{\mu} \beta_{\mu} \tilde{\rho}_{\mu}(\mathbf{r}), \quad (18)$$

where $\tilde{\rho}_{\mu} = K * \rho_{\mu}$, β_{μ} is the production rate of c by species μ , and K is the Green's function corresponding to the linear transport and degradation of the chemicals. For the sake of simplicity, we only consider biases on the self-propulsion speeds and set $v_{0\mu} \equiv v_0$, $\tau_{0\mu} \equiv \tau_0$ and $\tau_{1\mu}^{-1} = 0$ for all species. In the particle dynamics, chemotactic interactions can then be seen as ‘‘generalized’’ pairwise forces:

$$\dot{\mathbf{r}}_{i,\mu} = v_0 \mathbf{u}_{i,\mu} + \sum_{j,\nu} \mathbf{f}_{i,\mu}^{j,\nu},$$

where $\mathbf{f}_{i,\mu}^{j,\nu} = v_{1\mu} \beta_{\nu} \mathbf{u}_{i,\mu} [\mathbf{u}_{i,\mu} \cdot \nabla_{\mathbf{r}_{i,\mu}} K(\mathbf{r}_{i,\mu} - \mathbf{r}_{j,\nu})]$. (19)

We stress that $\mathbf{f}_{i,\mu}^{j,\nu}$ and $\mathbf{f}_{j,\nu}^{i,\mu}$ are not collinear, since $\mathbf{f}_{i,\mu}^{j,\nu}$ is directed along $\mathbf{u}_{i,\mu}$. The dynamics thus explicitly violates Newton's third law at the microscopic scale. Nevertheless, Eq. (17) ensures that reciprocity is restored at the coarse-grained scale whenever $v_{1\mu} \beta_{\nu} = v_{1\nu} \beta_{\mu}$ for all species. We note that equilibrium limits of chemotactic [77, 78] or diffusiophoretic dynamics [12, 15, 20] have attracted a long-standing interest in the literature. Previous results, however, relied on microscopic Langevin dynamics in which chemotactic interactions enter directly as effective pairwise *collinear* forces, $\mathbf{f}_i^j \propto \nabla_i G(\mathbf{r}_i - \mathbf{r}_j)$ for some function G . The existence of macroscopic equilibrium limits then relies on imposing Newton's third law at the microscopic scale. On the contrary, Eq. (17) is, to the best of our knowledge, the first condition for chemotactic mixtures to recover reciprocity at the macroscopic scale, despite being non-reciprocal at the microscopic one.

DISCUSSION.

In this article we have shown how microscopic and macroscopic scales can be quantitatively bridged for a large class of active mixtures in the presence of mediated non-reciprocal interactions. This revealed a subtle and important property of non-reciprocity: it varies strongly across scales. Based on

this insight we derived non-trivial conditions on the *microscopic* NRI that lead to effective equilibrium at the *macroscopic* scale. This allowed us to account—accurately and without fit parameters—for the full range of static patterns observed in our simulations. Finally, we derived conditions for NRI to survive coarse-graining, hence leading to positive entropy production rate at the macroscopic scale. When non-reciprocity is strong enough, we showed the emergence of a wealth of dynamical patterns. Again, our micro-to-macro approach allows us to predict the phase diagram from microscopies without fitting parameters.

From a biophysical perspective, our study shows how QS and chemotactic interactions lead to a rich phenomenology in complex assemblies of cells. In the context of bacterial colonies, motility-induced patterns will eventually interact with population dynamics [57, 79, 80] and genetics [81]. How this interplay will result in diverse co-existing communities is a fascinating research direction for the future indeed.

Finally, turning synthetic active-matter systems into smart materials will require quantitative control over complex assemblies of active constituents. Our work demonstrates that one can go up the complexity ladder while retaining an analytical framework to account for the emerging properties of active systems. How these systems can then be optimized to accomplish given tasks is an exciting challenge that appears within reach, given recent progress in automatic differentiation [82].

Acknowledgment: JT acknowledges the financial support of ANR Thema. AD acknowledges an international fellowship from IDEX Universit e de Paris. PS acknowledges support by a RSE Saltire Facilitation Network Award. YZ acknowledges support from start-up grant NH10800621 from Soochow University.

-
- [1] O'Byrne, J., Kafri, Y., Tailleur, J. & van Wijland, F. Time irreversibility in active matter, from micro to macro. *Nature Reviews Physics* **4**, 167–183 (2022).
 - [2] Deseigne, J., Dauchot, O. & Chat e, H. Collective motion of vibrated polar disks. *Physical review letters* **105**, 098001 (2010).
 - [3] Schaller, V., Weber, C., Semmrich, C., Frey, E. & Bausch, A. R. Polar patterns of driven filaments. *Nature* **467**, 73–77 (2010).
 - [4] Sumino, Y. *et al.* Large-scale vortex lattice emerging from collectively moving microtubules. *Nature* **483**, 448–452 (2012).
 - [5] Bricard, A., Caussin, J.-B., Desreumaux, N., Dauchot, O. & Bartolo, D. Emergence of macroscopic directed motion in populations of motile colloids. *Nature* **503**, 95–98 (2013).
 - [6] Theurkauff, I., Cottin-Bizonne, C., Palacci, J., Ybert, C. & Bocquet, L. Dynamic clustering in active colloidal suspensions with chemical signaling. *Physical review letters* **108**, 268303 (2012).
 - [7] Palacci, J., Sacanna, S., Steinberg, A. P., Pine, D. J. & Chaikin, P. M. Living crystals of light-activated colloidal surfers. *Science* **339**, 936–940 (2013).
 - [8] Buttinoni, I. *et al.* Dynamical clustering and phase separation in suspensions of self-propelled colloidal particles. *Physical review letters* **110**, 238301 (2013).
 - [9] van der Linden, M. N., Alexander, L. C., Aarts, D. G. &

- Dauchot, O. Interrupted motility induced phase separation in aligning active colloids. *Physical Review Letters* **123**, 098001 (2019).
- [10] Tan, T. H. *et al.* Odd dynamics of living chiral crystals. *Nature* **607**, 287–293 (2022).
- [11] Marchetti, M. C. *et al.* Hydrodynamics of soft active matter. *Reviews of Modern Physics* **85**, 1143–1189 (2013).
- [12] Soto, R. & Golestanian, R. Self-assembly of catalytically active colloidal molecules: Tailoring activity through surface chemistry. *Physical Review Letters* **112**, 068301 (2014).
- [13] Baek, Y., Solon, A. P., Xu, X., Nikola, N. & Kafri, Y. Generic long-range interactions between passive bodies in an active fluid. *Physical review letters* **120**, 058002 (2018).
- [14] Saha, S., Ramaswamy, S. & Golestanian, R. Pairing, waltzing and scattering of chemotactic active colloids. *New Journal of Physics* **21**, 063006 (2019).
- [15] Agudo-Canalejo, J. & Golestanian, R. Active phase separation in mixtures of chemically interacting particles. *Physical Review Letters* **123**, 018101 (2019).
- [16] Saha, S., Agudo-Canalejo, J. & Golestanian, R. Scalar active mixtures: The nonreciprocal cahn-hilliard model. *Physical Review X* **10**, 041009 (2020).
- [17] You, Z., Baskaran, A. & Marchetti, M. C. Nonreciprocity as a generic route to traveling states. *Proceedings of the National Academy of Sciences* **117**, 19767–19772 (2020).
- [18] Nasouri, B. & Golestanian, R. Exact phoretic interaction of two chemically active particles. *Physical Review Letters* **124**, 168003 (2020).
- [19] Granek, O., Baek, Y., Kafri, Y. & Solon, A. P. Bodies in an interacting active fluid: far-field influence of a single body and interaction between two bodies. *Journal of Statistical Mechanics: Theory and Experiment* **2020**, 063211 (2020).
- [20] Ouazan-Reboul, V., Agudo-Canalejo, J. & Golestanian, R. Non-equilibrium phase separation in mixtures of catalytically active particles: size dispersity and screening effects. *The European Physical Journal E* **44**, 113 (2021).
- [21] Fruchart, M., Hanai, R., Littlewood, P. B. & Vitelli, V. Non-reciprocal phase transitions. *Nature* **592**, 363–369 (2021).
- [22] Frohoff-Hülsmann, T., Wrembel, J. & Thiele, U. Suppression of coarsening and emergence of oscillatory behavior in a cahn-hilliard model with nonvariational coupling. *Physical Review E* **103**, 042602 (2021).
- [23] Frohoff-Hülsmann, T. & Thiele, U. Localized states in coupled cahn-hilliard equations. *IMA Journal of Applied Mathematics* **86**, 924–943 (2021).
- [24] Poncet, A. & Bartolo, D. When soft crystals defy newton’s third law: Nonreciprocal mechanics and dislocation motility. *Physical Review Letters* **128**, 048002 (2022).
- [25] Gupta, R. K., Kant, R., Soni, H., Sood, A. K. & Ramaswamy, S. Active nonreciprocal attraction between motile particles in an elastic medium. *Phys. Rev. E* **105**, 064602 (2022).
- [26] Cross, M. C. & Hohenberg, P. C. Pattern formation outside of equilibrium. *Reviews of modern physics* **65**, 851 (1993).
- [27] Saarloos, W., Hecke, M., Hohenberg, P. & Natuurwetenschappen, F. d. W. e. Amplitude equations for pattern forming systems (1994).
- [28] Aranson, I. S. & Kramer, L. The world of the complex ginzburg-landau equation. *Reviews of modern physics* **74**, 99 (2002).
- [29] Rapp, L., Bergmann, F. & Zimmermann, W. Systematic extension of the cahn-hilliard model for motility-induced phase separation. *The European Physical Journal E* **42**, 1–10 (2019).
- [30] Bergmann, F., Rapp, L. & Zimmermann, W. Active phase separation: A universal approach. *Physical Review E* **98**, 020603 (2018).
- [31] Stenhammar, J., Wittkowski, R., Marenduzzo, D. & Cates, M. E. Activity-induced phase separation and self-assembly in mixtures of active and passive particles. *Physical review letters* **114**, 018301 (2015).
- [32] Yeo, K., Lushi, E. & Vlahovska, P. M. Collective dynamics in a binary mixture of hydrodynamically coupled microrotors. *Physical review letters* **114**, 188301 (2015).
- [33] Wysocki, A., Winkler, R. G. & Gompper, G. Propagating interfaces in mixtures of active and passive brownian particles. *New journal of physics* **18**, 123030 (2016).
- [34] Wittkowski, R., Stenhammar, J. & Cates, M. E. Nonequilibrium dynamics of mixtures of active and passive colloidal particles. *New Journal of Physics* **19**, 105003 (2017).
- [35] Stürmer, J., Seyrich, M. & Stark, H. Chemotaxis in a binary mixture of active and passive particles. *The Journal of chemical physics* **150**, 214901 (2019).
- [36] Rodriguez, D. R., Alarcon, F., Martinez, R., Ramirez, J. & Valeriani, C. Phase behaviour and dynamical features of a two-dimensional binary mixture of active/passive spherical particles. *Soft Matter* **16**, 1162–1169 (2020).
- [37] Kolb, T. & Klotsa, D. Active binary mixtures of fast and slow hard spheres. *Soft Matter* **16**, 1967–1978 (2020).
- [38] Bárdfalvy, D., Anjum, S., Nardini, C., Morozov, A. & Stenhammar, J. Symmetric mixtures of pusher and puller microswimmers behave as noninteracting suspensions. *Physical Review Letters* **125**, 018003 (2020).
- [39] de Castro, P., Diles, S., Soto, R. & Sollich, P. Active mixtures in a narrow channel: Motility diversity changes cluster sizes. *Soft Matter* **17**, 2050–2061 (2021).
- [40] de Castro, P., Rocha, F. M., Diles, S., Soto, R. & Sollich, P. Diversity of self-propulsion speeds reduces motility-induced clustering in confined active matter. *Soft Matter* **17**, 9926–9936 (2021).
- [41] Paoluzzi, M., Leoni, M. & Marchetti, M. C. Information and motility exchange in collectives of active particles. *Soft Matter* **16**, 6317–6327 (2020).
- [42] Li, Y. I. & Cates, M. E. Hierarchical microphase separation in non-conserved active mixtures. *The European Physical Journal E* **44**, 1–8 (2021).
- [43] Williams, S., Jeanneret, R., Tuval, I. & Polin, M. Confinement-induced accumulation and spontaneous demixing of microscopic active-passive mixtures. *arXiv preprint arXiv:2111.09763* (2021).
- [44] Miller, M. B. & Bassler, B. L. Quorum sensing in bacteria. *Annual Review of Microbiology* **55**, 165–199 (2001).
- [45] Nealson, K. H., Platt, T. & Hastings, J. W. Cellular control of the synthesis and activity of the bacterial luminescent system. *Journal of Bacteriology* **104**, 313–322 (1970).
- [46] Engebrecht, J. & Silverman, M. Identification of genes and gene products necessary for bacterial bioluminescence. *Proceedings of the National Academy of Sciences* **81**, 4154–4158 (1984).
- [47] Fuqua, W. C., Winans, S. C. & Greenberg, E. P. Quorum sensing in bacteria: the luxR-luxI family of cell density-responsive transcriptional regulators. *Journal of bacteriology* **176**, 269–275 (1994).
- [48] Verma, S. C. & Miyashiro, T. Quorum sensing in the squid-vibrio symbiosis. *International journal of molecular sciences* **14**, 16386–16401 (2013).
- [49] Tsou, A. M. & Zhu, J. Quorum sensing negatively regulates hemolysin transcriptionally and posttranslationally in *Vibrio cholerae*. *Infection and Immunity* **78**, 461–467 (2010).
- [50] Hammer, B. K. & Bassler, B. L. Quorum sensing controls

- biofilm formation in vibrio cholerae. *Molecular Microbiology* **50**, 101–104 (2003).
- [51] Daniels, R., Vanderleyden, J. & Michiels, J. Quorum sensing and swarming migration in bacteria. *FEMS Microbiology Reviews* **28**, 261–289 (2004).
- [52] Bäuerle, T., Fischer, A., Speck, T. & Bechinger, C. Self-organization of active particles by quorum sensing rules. *Nature Communications* **9**, 3232 (2018).
- [53] Lavergne, F. A., Wendehenne, H., Bäuerle, T. & Bechinger, C. Group formation and cohesion of active particles with visual perception-dependent motility. *Science* (2019).
- [54] Massana-Cid, H., Maggi, C., Frangipane, G. & Di Leonardo, R. Rectification and confinement of photokinetic bacteria in an optical feedback loop. *Nature Communications* **13**, 2740 (2022).
- [55] Note that making $\tau_{i,\mu}$ a function of \mathbf{r}_i and a functional of $\{\rho_\nu\}$ does not lead to any interesting phenomenology so, for simplicity, we do not consider this case in the main text.
- [56] Hohenberg, P. C. & Halperin, B. I. Theory of dynamic critical phenomena. *Reviews of Modern Physics* **49**, 435–479 (1977).
- [57] Curatolo, A. I. *et al.* Cooperative pattern formation in multi-component bacterial systems through reciprocal motility regulation. *Nature Physics* **16**, 1152–1157 (2020).
- [58] O’Byrne, J. & Tailleur, J. Lamellar to micellar phases and beyond: When tactic active systems admit free energy functionals. *Physical Review Letters* **125**, 208003 (2020).
- [59] Cates, M. E. & Tailleur, J. Motility-induced phase separation. *Annual Review of Condensed Matter Physics* **6**, 219–244 (2015).
- [60] Fodor, É. & Marchetti, M. C. The statistical physics of active matter: From self-catalytic colloids to living cells. *Physica A: Statistical Mechanics and its Applications* **504**, 106–120 (2018).
- [61] Sollich, P. Predicting phase equilibria in polydisperse systems. *Journal of Physics: Condensed Matter* **14**, R79–R117 (2001).
- [62] Cross, M. C. & Hohenberg, P. C. Pattern formation outside of equilibrium. *Reviews of Modern Physics* **65**, 851–1112 (1993).
- [63] Schnitzer, M. J. Theory of continuum random walks and application to chemotaxis. *Phys. Rev. E* **48**, 2553–2568 (1993).
- [64] Tailleur, J. & Cates, M. E. Statistical mechanics of interacting run-and-tumble bacteria. *Physical Review Letters* **100**, 218103 (2008).
- [65] Cates, M. E. & Tailleur, J. When are active brownian particles and run-and-tumble particles equivalent? consequences for motility-induced phase separation. *EPL - Europhysics Letters* **101**, 20010 (2013).
- [66] Martin, D. *et al.* Statistical mechanics of active ornstein-uhlenbeck particles. *Phys. Rev. E* **103**, 032607 (2021).
- [67] Frangipane, G. *et al.* Dynamic density shaping of photokinetic e. coli. *eLife* **7**, e36608 (2018).
- [68] Arlt, J., Martinez, V. A., Dawson, A., Pilizota, T. & Poon, W. C. K. Painting with light-powered bacteria. *Nat Commun* **9**, 768 (2018).
- [69] Berg, H. C. Chemotaxis in bacteria. *Annual review of biophysics and bioengineering* **4**, 119–136 (1975).
- [70] Budrene, E. O. & Berg, H. C. Dynamics of formation of symmetrical patterns by chemotactic bacteria. *Nature* **376**, 49–53 (1995).
- [71] Woodward, D. E. *et al.* Spatio-temporal patterns generated by salmonella typhimurium. *Biophysical journal* **68**, 2181–2189 (1995).
- [72] Brenner, M. P., Levitov, L. S. & Budrene, E. O. Physical mechanisms for chemotactic pattern formation by bacteria. *Biophysical journal* **74**, 1677–1693 (1998).
- [73] Saragosti, J. *et al.* Directional persistence of chemotactic bacteria in a traveling concentration wave. *Proceedings of the National Academy of Sciences* **108**, 16235–16240 (2011).
- [74] Chatterjee, S., da Silveira, R. A. & Kafri, Y. Chemotaxis when bacteria remember: drift versus diffusion. *PLoS computational biology* **7**, e1002283 (2011).
- [75] Sourjik, V. & Wingreen, N. S. Responding to chemical gradients: bacterial chemotaxis. *Current opinion in cell biology* **24**, 262–268 (2012).
- [76] Cremer, J. *et al.* Chemotaxis as a navigation strategy to boost range expansion. *Nature* **575**, 658–663 (2019).
- [77] Newman, T. & Grima, R. Many-body theory of chemotactic cell-cell interactions. *Physical Review E* **70**, 051916 (2004).
- [78] Chavanis, P.-H. Exact diffusion coefficient of self-gravitating brownian particles in two dimensions. *The European Physical Journal B* **57**, 391–409 (2007).
- [79] Cates, M. E., Marenduzzo, D., Pagonabarraga, I. & Tailleur, J. Arrested phase separation in reproducing bacteria creates a generic route to pattern formation. *Proceedings of the National Academy of Sciences* **107**, 11715–11720 (2010).
- [80] Liu, C. *et al.* Sequential establishment of stripe patterns in an expanding cell population. *Science* (2011).
- [81] Hallatschek, O., Hersen, P., Ramanathan, S. & Nelson, D. R. Genetic drift at expanding frontiers promotes gene segregation. *Proceedings of the National Academy of Sciences* **104**, 19926–19930 (2007).
- [82] Goodrich, C. P., King, E. M., Schoenholz, S. S., Cubuk, E. D. & Brenner, M. P. Designing self-assembling kinetics with differentiable statistical physics models. *Proceedings of the National Academy of Sciences* **118**, e2024083118 (2021).